

Numerical simulation of viscid flow around hydrofoil

Paweł Dymarski

Ship Design and Research Centre – Stock Company, Gdańsk

ABSTRACT



This paper presents results of application of a viscid fluid model to calculate flow around a finite-span hydrofoil. The presented calculations were performed with the use of SOLAGA software developed by this author. The used theoretical model of viscid liquid motion was described, consisted of averaged liquid motion equations and Spalart-Allmaras one-equation model of turbulence. Also, a numerical model based on the finite volume method was shortly presented. Calculation results were shown in the form of distribution diagrams of pressures, longitudinal component of velocity and longitudinal component of rotation velocity. Additionally, the presented characteristics of the lifting force coefficient and drag force coefficient were compared with experimental data.

Keywords : viscid flow around hydrofoil, Spalart-Allmaras model, Finite Volume Method, SOLAGA

INTRODUCTION

Hydromechanical calculations of ship screw propellers carried out by Polish research centres (Ship Design and Research Centre – Stock Company, Institute of Fluid Flow Machinery - Polish Academy of Sciences, and Gdańsk University of Technology) are mainly based on potential motion of liquid, i.e. such as used in vortex methods or surface panel methods. In recent years in shipbuilding have been often and often applied programs dealing with viscid liquid flow. The programs are based on the Reynolds Averaged Navier-Stokes Equation (RANSE) and turbulence model equations. Solvers based on the RANSE methods have been for years applied to calculate ship wake, and quite recently they have been used as „universal” programs for solving any hydromechanical problem.

The project under development, whose partial results have been presented in this paper, is aimed at elaboration of an algorithm and computer program for calculating the viscid flow around ship propellers and hydrofoils. This author is convinced that development of a computer program specialized in calculating objects of one kind will make it possible to obtain - in the future - better results against those achievable from the „universal” solvers widely applied (mainly abroad).

In this paper are presented calculation results obtained by means of the SOLAGA computer software under development within the frame of the project in question. The test calculations were performed for a rectangular hydrofoil of NACA66-9 profile and the aspect ratio $\Lambda = 6$.

VISCID FLUID MOTION EQUATIONS

The closed system of fluid motion equations is based on two principles : the principle of mass conservation and principle of conservation of momentum.

The equation of mass conservation formulated for inviscid fluid is as follows :

$$\frac{\partial \mathbf{u}_i}{\partial x_i} = 0 \quad (1)$$

And the equation of conservation of momentum has the following form :

$$\rho \frac{\partial \mathbf{u}_i}{\partial t} + \rho \mathbf{u}_i \frac{\partial \mathbf{u}_i}{\partial x_j} = - \frac{\partial p}{\partial x_i} + \frac{\partial}{\partial x_j} (2\mu s_{ji}) \quad (2)$$

where :

$$s_{ji} = \frac{1}{2} \left(\frac{\partial u_j}{\partial x_i} + \frac{\partial u_i}{\partial x_j} \right) \quad (3)$$

is the strain - rate tensor and :

- p - pressure
- ρ - density
- μ - dynamic viscosity coefficient
- x_i, u_i - components of location vector and velocity vector, respectively.

The above given equations fully describing the behaviour of Newtonian incompressible liquid are applicable in calculating the flows characterized by small values of Reynolds number, i.e. up to about $10^3 \div 10^4$.

In the case of flows of a greater Reynolds number, to apply the equations is not possible due to the scale of phenomena occurring in the fluid.

In the engineering problems associated with flow of water, Reynolds numbers as usual greatly exceed the value of 10^4 . In ship hydromechanics its value is as a rule contained within the interval of $10^6 \div 10^8$, and in this connection instead of Eqs (1) and (2) their averaged equivalents are used.

The instantaneous velocity vector $u_i(x,t)$ can be presented as a sum of the average velocity $U_i(x)$ and the fluctuation $u'_i(x,t)$:

$$u_i(x,t) = U_i(x) + u'_i(x,t) \quad (4)$$

In a similar way the instantaneous pressure field $p(x,t)$ can be described:

$$p(x,t) = P(x) + p'(x,t) \quad (5)$$

Applying the above notation used to the set of Eqs (1),(2) one obtains the averaged equations of motion [6]:

$$\frac{\partial U_i}{\partial x_i} = 0 \quad (6)$$

$$\rho \frac{\partial U_i}{\partial t} + \rho U_i \frac{\partial U_i}{\partial x_j} = - \frac{\partial P}{\partial x_i} + \frac{\partial}{\partial x_j} (2\mu S_{ji} - \overline{\rho u'_j u'_i}) \quad (7)$$

In the averaged momentum conservation equation the term $-\overline{\rho u'_i u'_j}$ (called *Reynolds stress tensor*) appears. In order to compute the tensor it is necessary to introduce additional equations which are called *turbulence model*. A turbulence model is selected respective to a considered kind of flow and an assumed calculation accuracy; calculation time is also one of the important factors - the more complex model the longer time of calculations.

In the presented calculation program the Spalart-Allmaras one-equation model was used, introduced for calculating hydrofoils.

The turbulent stress tensor is calculated on the basis of Bousinesq's hypothesis which assumes that the Reynolds stresses can be expressed by means of the turbulent viscosity and mean strain - rate tensor:

$$\tau_{ij} = \overline{\rho u'_i u'_j} = \rho \nu_T \left(\frac{\partial U_i}{\partial x_j} + \frac{\partial U_j}{\partial x_i} \right) \quad (8)$$

The kinematic turbulent viscosity ν_T is calculated from the formula:

$$\nu_T = \tilde{\nu} f_{v1} \quad (9)$$

And, the modified turbulent viscosity $\tilde{\nu}$ is calculated with the use of the transport equation:

$$\frac{\partial \tilde{\nu}}{\partial t} + U_j \frac{\partial \tilde{\nu}}{\partial x_j} = c_{b1} \tilde{S}_{SA} \tilde{\nu} - c_{w1} f_w \left(\frac{\tilde{\nu}}{d} \right)^2 + \frac{1}{\sigma} \frac{\partial}{\partial x_k} \left[(\nu + \tilde{\nu}) \frac{\partial \tilde{\nu}}{\partial x_k} \right] + \frac{c_{b2}}{\sigma} \frac{\partial \tilde{\nu}}{\partial x_k} \frac{\partial \tilde{\nu}}{\partial x_k} \quad (10)$$

The values of the model's coefficients and the relations between the coefficients are given below:

$$c_{b1} = 0.1355, \quad c_{b2} = 0.622, \quad c_{v1} = 7.1, \quad \sigma = 2/3 \quad (11)$$

$$c_{w1} = \frac{c_{b1}}{\kappa^2} + \frac{1 + c_{b2}}{\sigma} \quad (12)$$

$$c_{w2} = 0.3, \quad c_{w3} = 2, \quad \kappa = 0.41$$

$$f_{v1} = \frac{\chi^3}{\chi^3 + c_{v1}^3}, \quad f_{v2} = 1 - \frac{\chi}{1 + \chi f_{v1}} \quad (13)$$

$$f_w = g \left[\frac{1 + c_{w3}^6}{g^6 + c_{w3}^6} \right]^{1/6}$$

$$\chi = \frac{\tilde{\nu}}{\nu}, \quad g = r + c_{w2} (r^6 - r), \quad r = \frac{\tilde{\nu}}{\tilde{S}_{SA} \kappa^2 d^2} \quad (14)$$

$$\tilde{S}_{SA} = S_{SA} + \frac{\tilde{\nu}}{\kappa^2 d^2} f_{v2}, \quad S_{SA} = \sqrt{2\Omega_{ij}\Omega_{ij}} \quad (15)$$

where:

Ω_{ij} - rotation tensor

d - distance to the nearest surface of the flow-around object.

$$\Omega_{ij} = \frac{1}{2} \left(\frac{\partial U_i}{\partial x_j} - \frac{\partial U_j}{\partial x_i} \right) \quad (16)$$

The assumed initial and boundary conditions

The value of the modified turbulent viscosity $\tilde{\nu}$ equal to 0.1ν (where: ν - coefficient of molecular kinematic viscosity) was assumed at inlet. On the hydrofoil surface $\tilde{\nu} = 0$ is assumed as the turbulent viscosity in the flow close to wall amounts to zero. [2].

NUMERICAL MODEL

The below presented equations are solved in a discrete way - they are transformed into a set of algebraic equations formulated for each node of calculation grid. Depending on specificity of a considered problem one can use one of the following space discretization method:

- Finite Differences Method (FDM) [4]
- Finite Element Method (FEM) [3]
- Finite Volume Method (FVM) [4].

In the SOLAGA software the discretization is performed by means of the FVM which provides a great freedom in selecting a kind of calculation grid, that makes it possible to calculate flow around objects of complex geometry.

Discretization of computation space. The Finite Volume Method (FVM)

The initial point to formulate the FV Method is the integral form of conservation equations, namely a considered calculation space is divided into a finite number of control volumes and for each of them relevant behaviour equations are formulated. Eq. (17) shows the general form of the conservation equation of the scalar quantity ϕ , given in the integral form:

$$\int_S \rho \phi \mathbf{V} \cdot \mathbf{n} dS = \int_S \Gamma \text{grad} \phi \cdot \mathbf{n} dS + \int_\Omega q_\phi d\Omega \quad (17)$$

where:

\mathbf{V} - velocity vector

ϕ - field scalar function

\mathbf{n} - vector normal to the control element surface S

Γ - diffusivity

q_ϕ - source of the quantity ϕ .

The surface and volume integrals appearing in the above given equation are calculated by means of approximate methods. Values of the field function between computation nodes are obtained by using interpolation.

Calculation of surface and volume integrals

The surface and volume integrals appearing in Eq. (17) are calculated by means of the below described quadratures.

The integral of the function f on the surface S can be developed as follows (Fig. 1) :

$$\int_S f dS = \sum_k \int_{S_k} f dS \tag{18}$$

where :

S_k - surface of the wall with the index k ($k = w, e, s, n, b, t$).

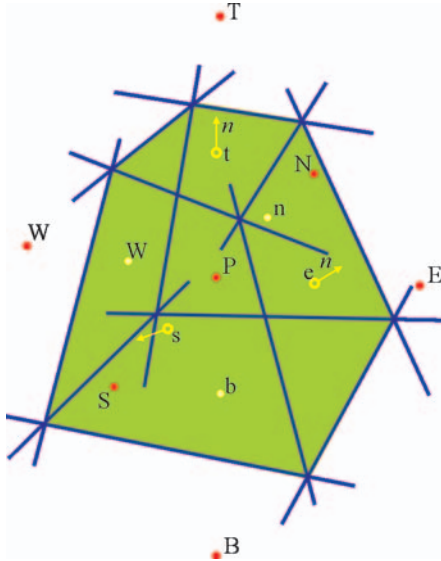


Fig. 1. Control element of 3D grid containing the node P . The nodes : W, E, S, N, B, T of the neighbouring elements and the central points of the element walls w, e, s, n, b, t are also depicted.

The integral of the function f on the single wall S_e is approximately calculated by applying the central point method :

$$\int_{S_e} f dS \approx f_e S_e \tag{19}$$

where : f_e - value of the integrand in the central point e of the surface S_e .

The volume integrals are calculated in an analogical way; the integral of the field function q over the volume Ω can be calculated as follows :

$$Q_P = \int_{\Omega} q d\Omega \approx q_P \Omega \tag{20}$$

where : q_P - value of the function q in the central point P .

Field function values in the central points of control volumes (nodes) are obtained directly from solving the set of equations, whereas field function values on the control volume surface are calculated by means of appropriate interpolation schemes.

Interpolation schemes

Carrying out calculations with the use of SOLAGA software one can apply two kinds of interpolation schemes :

- ★ **Upwind** interpolation (UDS)
- ★ **Linear** interpolation (CDS).

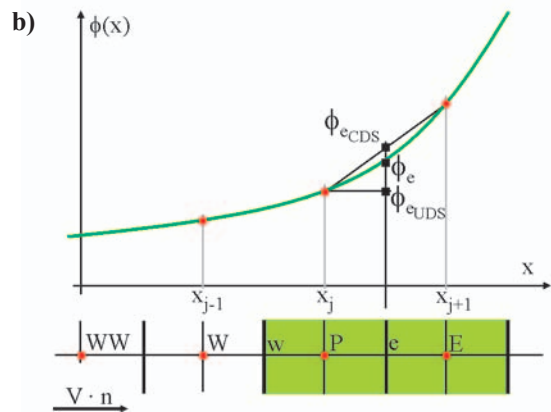
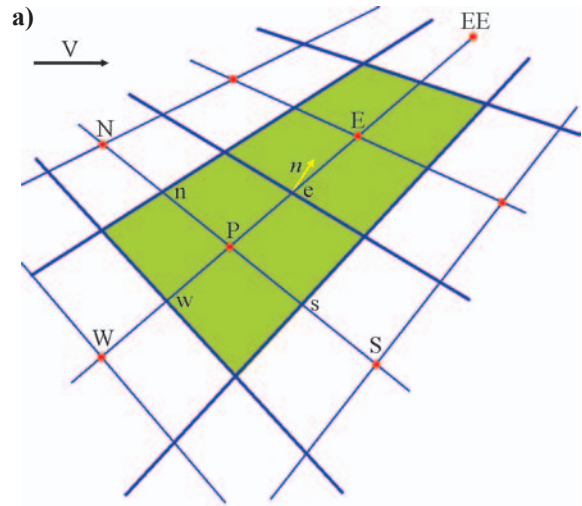


Fig. 2.a) Cross-section through 3D calculation grid. **Note :** control elements with the nodes P and E and the wall located between them and containing the central point e , are marked grey. Value of the function ϕ in this point is obtained by using interpolation.

In Fig. 2.b) are shown principles of operation of the interpolation schemes: UDS – upwind interpolation, CDS – linear interpolation.

In the *upwind* method, transport of the medium described by the function ϕ is assumed to be realized mainly by convection – value of the function in the central point of the element’s wall is equal to that in the neighbouring node located „upwind” the medium flow. Value of the function ϕ in the point e (Fig.2) is calculated by using the following formula :

$$\phi_{e,UDS} = \begin{cases} \phi_P & \text{if } (\mathbf{V} \cdot \mathbf{n})_e > 0 \\ \phi_E & \text{if } (\mathbf{V} \cdot \mathbf{n})_e < 0 \end{cases} \tag{21}$$

The *upwind* scheme is unconditionally stable and does not lead to oscillating solutions. Its drawback consists in a large numerical diffusion and low accuracy (of 1st order).

More accurate results can be obtained by using the linear interpolation scheme (CDS) based on the assumption that the function between the points P and E varies linearly (Fig.2 b). Value of the function ϕ in the point e is calculated as follows :

$$\phi_{e,CDS} = \phi_E \lambda_e + \phi_P (1 - \lambda_e) \tag{22}$$

where : λ_e - linear interpolation coefficient calculated by means of the following formula :

$$\lambda_e = \frac{|x_e - x_P|}{|x_E - x_P|} \tag{23}$$

Eq. (22) is of the degree of 2nd-order accuracy. The CDS scheme is characterized by a much lower numerical diffusion than that of the *upwind* one. The drawback of the CDS scheme is its lower stability and susceptibility to generate oscillating solutions.

In order to avoid the solution instability the both schemes are connected together by introducing the so called blending factor $B \in \langle 0 ; 1 \rangle$. The interpolated value of the function ϕ in the point e is hence determined as follows :

$$\phi_e = (1 - B)\phi_{e,UDS} + B\phi_{e,CDS} \quad (24)$$

where :

$\phi_{e,UDS}$ - value calculated by means of the UDS scheme
 $\phi_{e,CDS}$ - value calculated by means of the CDS scheme.

This approach makes it possible to achieve a stable solution at maintaining a relatively high degree of calculation accuracy.

Numerical methods of solving non-stationary problems

In the case when considered problems have a non-stationary character it is necessary to apply the methods analogous to those used in solving initial problems for ordinary differential equations.

The problems associated with liquid flow are as a rule characterized by time-variability in spite of stationary boundary conditions, in the cases application of a non-stationary model is recommended. Such approach is especially justified in the case of calculation of rather non-streamlined objects where flow separation may occur.

Methods of solving initial problems of ordinary differential equations

After spatial discretization of the partial differential equation the set of ordinary differential equations is obtained in the following form :

$$\frac{d\vec{\phi}(t)}{dt} = \vec{F}[t, \vec{\phi}(t)] \quad , \quad \vec{\phi}(t_0) = \vec{\phi}^0 \quad (25)$$

The simplest way of solving the above given equation is its integration within consecutive time intervals to obtain the solution for the successive time values $t_1, t_2, t_3 \dots$

$$\int_{t_n}^{t_{n+1}} \frac{d\vec{\phi}(t)}{dt} dt = \vec{\phi}^{n+1} - \vec{\phi}^n = \int_{t_n}^{t_{n+1}} \vec{F}[t, \vec{\phi}(t)] dt \quad (26)$$

The above given expression is accurate. Numerical methods for determining the quantity $\vec{\phi}^{n+1}$ are classified with accounting for a way of calculation of the right-hand side integral. In the presented software two integration methods are applied : the *backward (implicit) Euler* method and *three time level* method. In the *Euler* method a value of the integrand within the whole interval $t \in \langle t_n, t_{n+1} \rangle$ is assumed equal to $\vec{F}[t_{n+1}, \vec{\phi}(t_{n+1})]$, see Fig.3a. Elements of the vector $\vec{\phi}$ in the successive time-step are calculated as follows :

$$\vec{\phi}^{n+1} = \vec{\phi}^n + \vec{F}(t_{n+1}, \vec{\phi}^{n+1})\Delta t \quad (27)$$

The *three time level* method consists in approximating the course of the function $\vec{F}[t_{n+1}, \vec{\phi}(t_{n+1})]$ by means of 2nd order parabola crossing the points t_{n-1}, t_n, t_{n+1} , see Fig.3b. The formula of the method is as follows :

$$\vec{\phi}^{n+1} = \frac{4}{3}\vec{\phi}^n - \frac{1}{3}\vec{\phi}^{n-1} + \frac{2}{3}\vec{F}(t_{n+1}, \vec{\phi}^{n+1})\Delta t \quad (28)$$

Both the mentioned methods are of implicit kind, i.e. that knowledge of values of its elements is necessary to calculate the vector $\vec{\phi}^{n+1}$. As a result of the application of one of the above described methods a set of m - equations is formed in every time step, where m stands for a number of calculation nodes. The equation set is solved in an iterative way by using the methods described below.

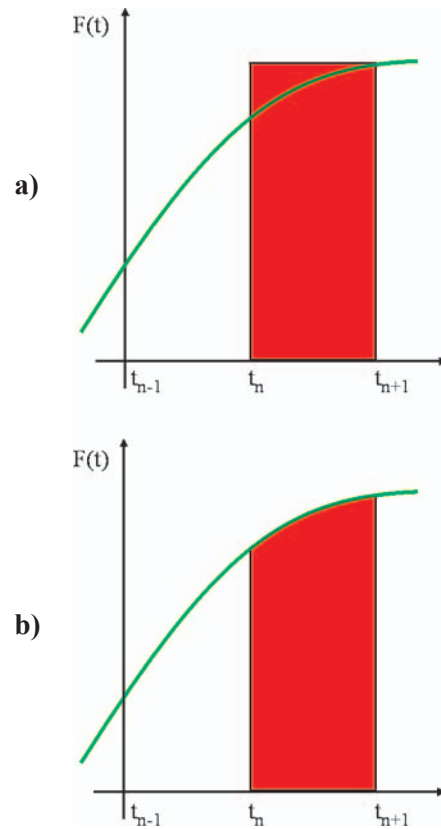


Fig. 3. Numerical integration of equations for non-stationary problems :
a) implicit Euler method, b) three time level method .

Methods of solving the sets of equations

As a result of spatial discretization of motion equations a set of algebraic equations formulated for each of the control volumes is obtained. The set, when linearized, is solved in an iterative way. In the software in question the algorithms based on the method of conjugate gradients are used : ICCG algorithm serves for solving the symmetrical matrices obtained from discretization of the Poisson equation (calculation of pressure corrections), and the unsymmetrical matrices are solved by means of Bi-CGSTAB algorithm. The above mentioned algorithms are described in [4].

TESTING CALCULATIONS

Computational data

The geometry of hydrofoil	Chord : $c = 0.2$ m Span : $w = 1.2$ m Profile : NACA 66-9
Angles of attack	0, 2, 4, 6, 8, 10, 12 degrees
Inflow velocity	$V = 5$ m/s

Model details

Turbulence model	Spalart-Allmaras (see Eqs 8 ÷ 16)
Interpolation scheme	UDS and CDS (blending factor $B = 0.5$)
Time integral approximation scheme	Implicit Euler (1 st order)
Time step	$0.002 \div 0.01$ sec
Number of control volumes	600 000

Results

Maps of pressure distribution on the hydrofoil plane of symmetry for various angles of attack are shown in Fig.4. And distribution of rotation in the wake behind the hydrofoil is shown in Fig.5. Distribution of the longitudinal component of rotation is presented in Fig.6.

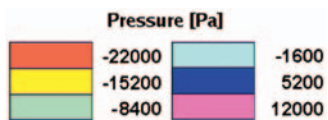
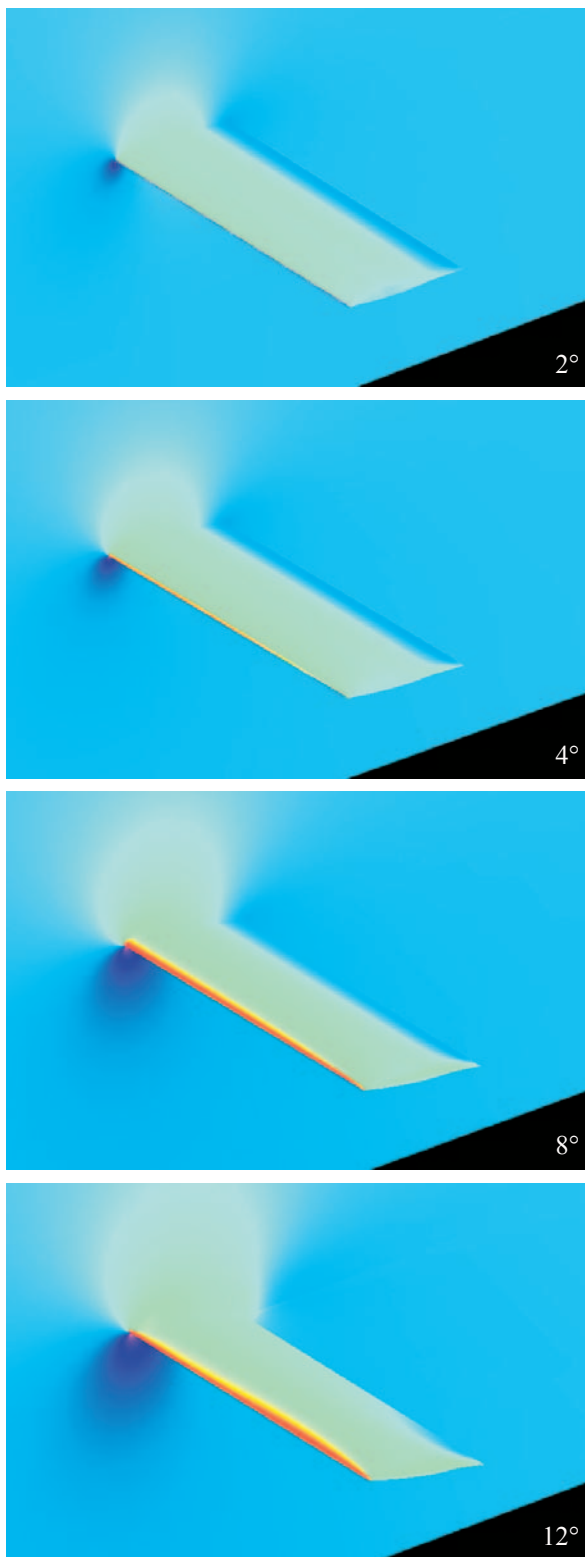


Fig. 4. Pressure distributions on surface of hydrofoil and its plane of symmetry .

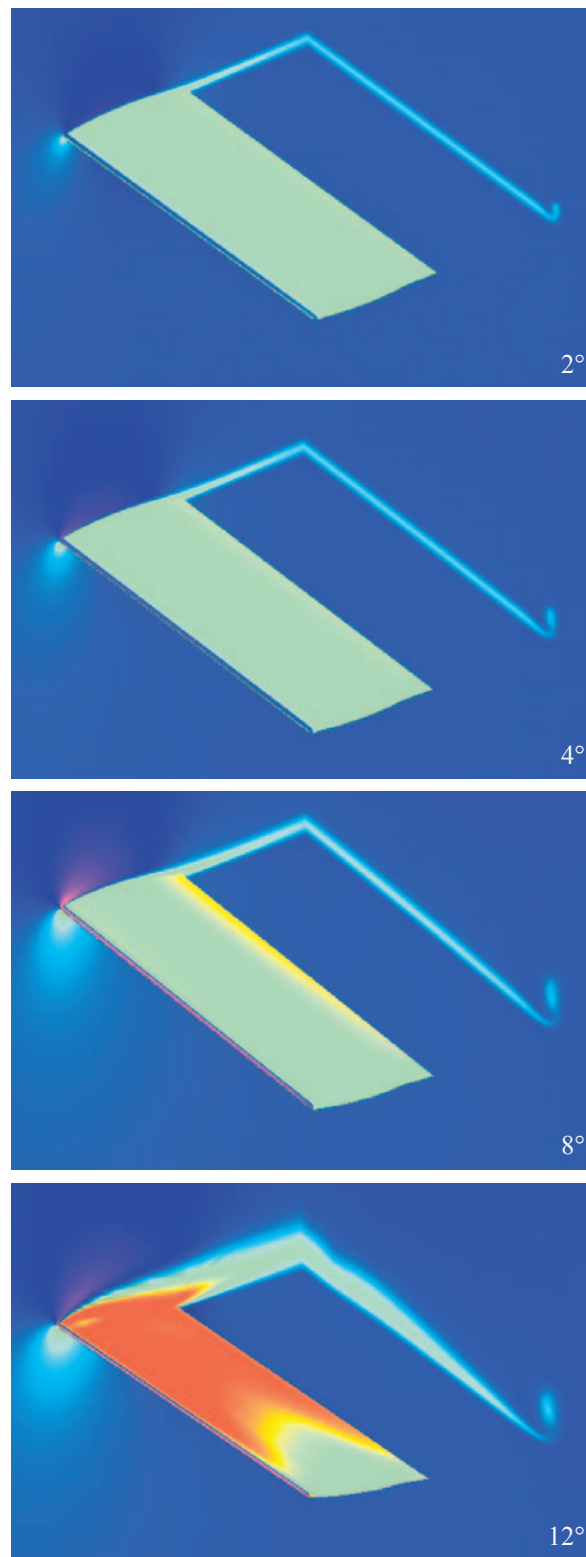


Fig. 5. Distribution of longitudinal velocity component just over hydrofoil's surface, in its plane of symmetry, and on the plane normal to flow direction, distant by one chord length behind trailing edge of the hydrofoil .

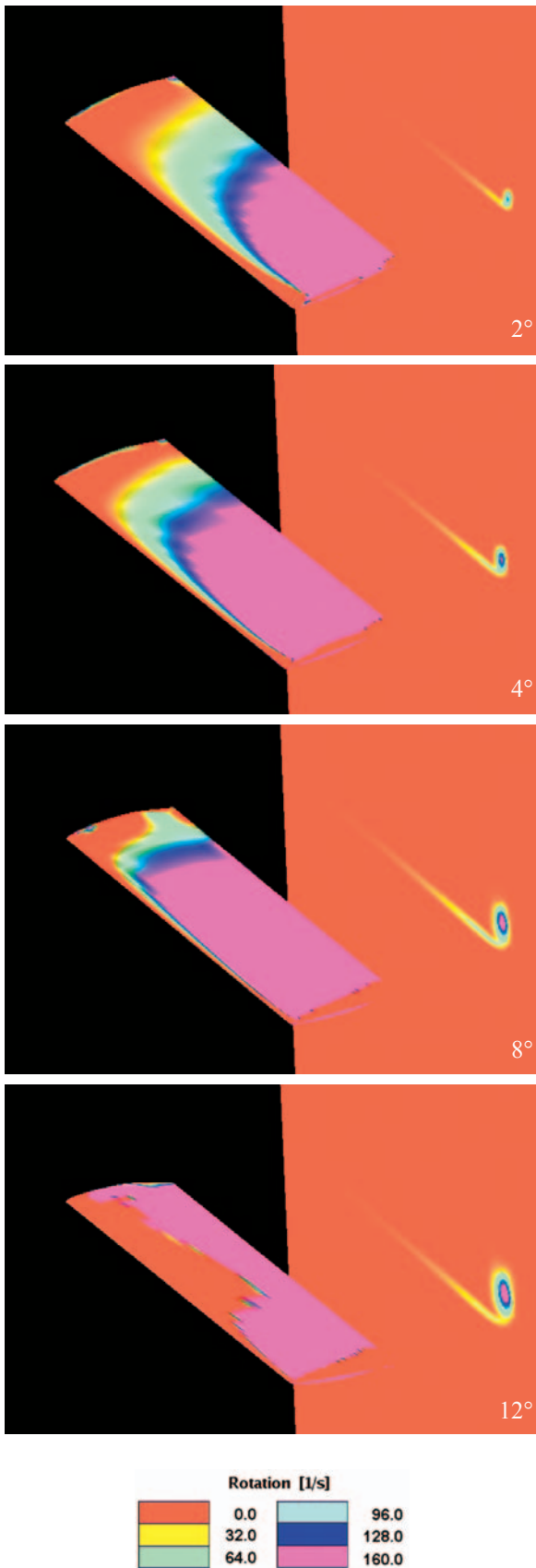


Fig. 6. Distribution of longitudinal rotational velocity component on the plane normal to flow direction, distant by one chord length behind trailing edge of the hydrofoil. The multi-colour „spot” on the right-hand side shows distribution of rotation in the tip vortex core.

The computational characteristics of the coefficients of lifting force and drag force are compared with the experimental data [1] in Fig.7.

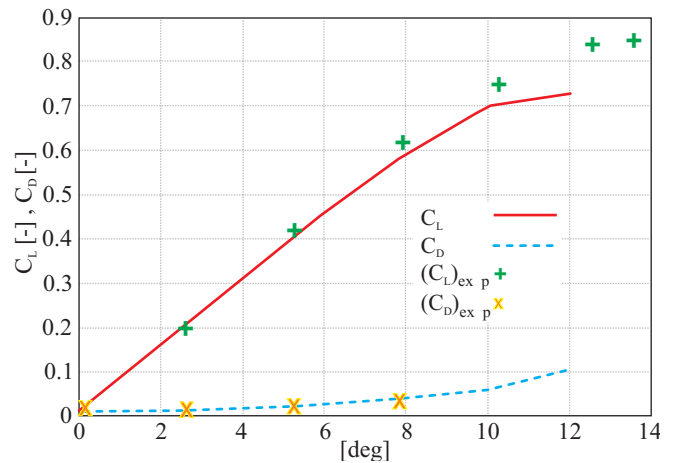


Fig. 7. Coefficients of the lifting force C_L and the drag force C_D in function of the angle of attack. The experimental data are in accordance with [1].

CONCLUSIONS

The computational results presented in this paper may be concluded as follows :

- The calculated pressure distribution around hydrofoil is qualitatively similar to that obtained from experiment.
- The calculated distribution of longitudinal component of rotation behind the hydrofoil is similar to the rotation fields obtained from the experiments [5]. The tip vortex core is clearly visible. The strength of vorticity increases up along with the angle of attack.
- The coefficients of lifting force and drag force are in a good conformity with the experimental data especially in the range of angle of attack from 0 to 6 degrees. The critical point of the lifting force coefficient characteristics is predicted with the accuracy of about $1 \div 2$ degrees.

Acknowledgement

The research presented in this paper has been financially supported by the Polish Ministry of Science and Information Society Technologies, (Grant No. 5 T12C 012 22). The author would like to express his gratitude for this support.

NOMENCLATURE

- C_D - drag force coefficient
- C_L - lifting force coefficient
- d - distance to the nearest surface of the flow - around object
- f - field function which determines a given (diffusional and/or convective) flow rate
- \vec{F} - vector of integrand functions of a set of ordinary differential equations (given in vectorial form)
- \mathbf{n} - vector normal to the surface S
- p - instantaneous pressure
- p' - pressure fluctuation
- P - time-averaged pressure
- q - function which determines field source
- Q_P - total source in control element containing the central point P
- S - control surface (which limits control element)
- S_{ji} - time-averaged strain - rate tensor of deformations
- t - time
- t_n - t value in n -th step of calculations
- u_i - instantaneous velocity component (in Cartesian notation)
- u'_i - fluctuation of velocity component
- U_i, U_j - time-averaged velocity components
- \mathbf{V} - velocity vector, see Eq.(17)
- x - location vector

x_i	- component of location vector
Γ	- diffusion coefficient of the quantity ϕ
μ	- dynamic viscosity coefficient of a liquid
ν	- kinematic viscosity coefficient of a liquid
$\bar{\nu}$	- turbulence model coefficient (turbulent modified viscosity), see Eq.(9)
ν_T	- kinematic turbulent viscosity coefficient of a liquid
ρ	- density
ϕ	- field scalar function
$\bar{\phi}$	- vector of ϕ function values in nodes of calculation grid (for a discrete form of ϕ function)
ϕ_e	- value of ϕ function in the point e
ϕ_E	- value of ϕ function in the point E
$\phi_{e,UDS}$	- value of ϕ_e approximated by using UDS scheme
$\phi_{e,CDS}$	- value of ϕ_e approximated by using CDS scheme
ϕ_p	- value of ϕ function in the point P
Ω	- control element volume.

Acronyms

Bi-CGSTAB	- BiConjugate Gradient Stabilized method
ICCG	- Incomplete Cholesky Conjugate Gradient method

BIBLIOGRAPHY

1. Abbott I.H., von Doenhoff A.E. : *Theory of Wing Sections*. Dover Publications inc. New York, 1959

2. Blazek J. : *Computational Fluid Dynamics: Principles and Applications*. ELSEVIER. 2001
3. Chung T.J. : *Computational Fluid Dynamics*. Cambridge University Press. 2002
4. Ferziger J.H., Peric M. : *Computational Methods for Fluid Dynamics*. Springer. Berlin, 1999
5. Koronowicz T. : *Rationality of Solving 3D Circulation Problems Exclusively with the Use of Navier-Stokes Equation*. TASK quarterly No 1/2002
6. Wilcox D.C. : *Turbulence Modeling for CFD*, DCW Industries. 2002 .

CONTACT WITH THE AUTHOR

Paweł Dymarski, M.Sc.,Eng.
 Ship Hydromechanics Division,
 Research and Development Department,
 Ship Design and Research Centre – Stock Company
 Szczecińska 65
 80-392 Gdańsk, POLAND
 e-mail : Pawel.Dymarski@cto.gda.pl

Conference



PTNSS Congress 2005



On 25–28 September 2005 was held 1st International Congress on Combustion Engines organized by Polish Scientific Society of Combustion Engines (PTNSS), under the slogan :

The development of combustion engines

The Congress in which representatives participated of universities and scientific research centres as well as automotive industry firms from 9 European countries, Japan and USA, took place in Bielsko-Biała, a town in the mountainous, south-western region of Poland.

Its program contained 3 plenary sessions with 4 papers presented during each of them, under the slogans :

Automotive/Engine Technology Development (4 papers)
Advanced Engine Design & Performance (8 papers)

and 5 technical sessions covering the following groups of topics :

- ✦ Engine testing (28 papers)
- ✦ Emission (17 papers)
- ✦ Fuel injection (9 papers)
- ✦ Combustion process (9 papers)
- ✦ Modeling (8 papers)
- ✦ Alternative fuels (6 papers)
- ✦ Various subjects (4 papers)

The third part was the poster session devoted to presentation of 42 different elaborations. Among so many different papers 9 of them dealt with ship engines, namely :

- ★ *Ways to improve operational properties of lorry engines* by Janusz Mysłowski and Jaromir Mysłowski (Technical University of Szczecin)

- ★ *Universal research test of toxic exhausts from ship piston engines* – by L. Piaseczny and T. Kniaziewicz (Polish Naval University)
- ★ *Possibilities of recognizing faults in gas turbine engines on the basis of simulation of transitory processes* – by A. Adamkiewicz (Polish Naval University) and M. Dzida (Gdańsk University of Technology)
- ★ *Analysis of vibration parameters of marine gas turbine engines* – by A. Grządziela (Polish Naval University)
- ★ *Diagnostic examination of marine engines in the Polish Navy* – by Z. Korczewski (Polish Naval University)
- ★ *Construction of modern valve train mechanism for marine diesel engines* – by T. Lus (Polish Naval University)
- ★ *Investigations of carbon deposits on injector nozzles of marine diesel engines* – by J. Monieta and P. Wójcikowski (Maritime University of Szczecin)
- ★ *Research on influence of delivery of water to cylinders on combustion process parameters and exhaust toxicity of internal combustion engines* – by L. Piaseczny and R. Zdrąg (Polish Naval University)
- ★ *Approximation of the cylinder compression pressure of the marine engine by means of a multi-parameter model* – by S. Polanowski (Polish Naval University)

Also, the panel discussion on „*Development trends of internal combustion engines*” was carried out within the frame of the Congress.



EXPLO-DIESEL & GAS TURBINE'05



On 9-13 May 2005 under this heading was held 4th International Scientific Technical Conference organized by the Faculty of Ocean Engineering & Ship Technology, Gdańsk University of Technology, together with MAN-B&W DIESEL A/S.

In accordance with the Conference slogan :

Keeping diesel engines and gas turbines in movement with regard to environmental protection

the Conference aim was to make science-practice relations closer and to participate in creation of a forum for exchange cognitive and utilitarian information on designing, manufacturing and operating the self-ignition engines and gas turbines as well as machines and other devices necessary to maintain the engines running, with special accounting for : their power and pro-ecological qualities as well as durability, reliability, diagnostics and operational safety.

The program's intentions were realized by 50 papers published in the Conference proceedings, 25 of which were presented and 20 were demonstrated during two poster sessions, as well as by 6 presentations performed by representatives of the companies working a.o. in the field of marine engineering, namely :

- *Marine diesel engines and catalytic fines – a new standard to ensure safe operation* – by G. Astroem (ALFA LAVAL)
- *Activity profile* – by Ł. Rózga (PBP ENAMOR Ltd)
- *ME engine concept in front of environment protection demands of today and in the future* – by S. Henningsen (MAN-B&W DIESEL A/S)

➤ *The latest MAN-B&W DIESEL design achievements on the base of S65ME-C engine concept* – by A. Oestergaard (MAN-B&W DIESEL A/S)

➤ *Application of portable electronic indicators in operation of self-ignition engines* – by L. Tomczak (UNITEST)

➤ *Application of 3D visualization in marine training software* – by L. Tomczak (UNITEST).

The course of the Conference was very attractive as four first sessions including one poster session were held in a hotel at Międzyzdroje, a health resort on the coast of the Baltic Sea, and the 5th session on board a ferry calling at Copenhagen where the 6th and 7th sessions were arranged in the MAN-B&W DIESEL headquarter.

There was also an occasion to visit a very interesting museum of the company and to be acquainted with running stand tests on the original 4T50MX two-stroke engine. Next day, after return to Międzyzdroje the last four sessions had place including one poster session.

Worth mentioning that the Conferences in question have been characterized traditionally by a very valuable consistency of theoretical knowledge and research and production practice.

Representatives of 16 scientific research and design centres took part in the preparation of papers for the Conference. The greatest share in this had scientific workers of Gdańsk University of Technology, Polish Naval University, Gdynia Maritime University, Poznań University of Technology, Airforce Technical Institute and Maritime University of Szczecin, who participated in the preparation of 12, 10, 7, 6, 4, and 3 papers, respectively.



MAN - B&W DIESEL - Copenhagen R&D centre